



## Microstructure evolution and properties of Cu–20Ni–20Mn alloy during aging process

Wei-bin XIE, Qiang-song WANG, Xu-jun MI, Guo-liang XIE, Dong-mei LIU, Xue-cheng GAO, Yang LI

State Key Laboratory for Fabrication and Processing of Non-ferrous Metals,  
General Research Institute for Nonferrous Metals, Beijing 100088, China

Received 17 November 2014; accepted 23 January 2015

**Abstract:** The microstructure evolution and phase transformation of Cu–20Ni–20Mn (mass fraction, %) alloy at 450 °C were investigated by X-ray diffraction and transmission electron microscopy (TEM). The variations of tensile strength, yield strength and hardness of this alloy during aging process were also analyzed. The results show that no significant variations of hardness and strength in the initial stage of aging, with a long incubation period, are observed at 450 °C. Subsequently, the ordered face-centered tetragonal (FCT) NiMn phase nucleates and grows up with prolonging the aging time. The hardness and tensile strength of the alloy increase up to their maximum values with increasing the ordered particle size, i.e., the strength of the alloy reaches 942 MPa after being aged at 450 °C for 40 h. The main cause of the age-hardening is considered to be precipitation strengthening due to the ordered FCT-NiMn particles.

**Key words:** Cu–Ni–Mn alloy; microstructure; mechanical properties; ordered phase

### 1 Introduction

Cu–Ni–Mn alloy has been widely used due to its high strength, high elasticity and good resistance to stress relaxation [1]. However, there is very limited understanding on the microstructural evolution in the aging process for Cu–Ni–Mn alloys. A new phase is precipitated in the grains and at the grain boundaries [2] when Cu–Ni–Mn alloy precipitation is hardened. RONDOT and MIGNOT [3] considered that high hardness of Cu–20Ni–20Mn alloy was achieved because of the development of FCT phase that grew rich in Ni–Mn, on the basis of the separation method of X-ray diffraction. Many researchers have investigated the phase diagram of the Cu–Ni–Mn system in very long time [4–9]. SUN et al [5] established a thermodynamic model for the Cu–Ni–Mn system. According to the thermodynamic model, Cu–20Ni–20Mn alloy consists of a  $\theta$ -MnNi phase with ordered  $L1_0$  structure and  $\gamma$ (Cu,Ni,Mn) with FCC structure in the temperature range of 300–500 °C. PAN [10] and SHAPIRO et al [11] found that the spinodal decomposition could take place during aging at 450 °C, the periodic structure appeared in

initial stage of the aging process, and coarsening of the periodic structure and its degeneration into the discrete ordered precipitates were obtained with continuing aging at this temperature. Nevertheless, the evidences of the spinodal decomposition process in the early stage of aging process are quite limited. The phase transformation of Cu–20Ni–20Mn (mass fraction, %) alloy during aging process is very complex. Thus, it is necessary to perform more detailed studies on the microstructure evolution of aging process. In this study, tensile test and hardness measurement, as well as X-ray diffraction and transmission electron microscopy, were used to investigate the mechanical properties and microstructural evolution of Cu–20Ni–20Mn alloy during aging process. The precipitation transformation during aging process and strengthening mechanism of Cu–20Ni–20Mn alloy were also discussed.

### 2 Experimental

Cu–20Ni–20Mn alloy was prepared by melting pure metals of Cu, Ni and Mn in a vacuum induction melting furnace. The ingot was subsequently hot-forged at 850 °C into a rod with a diameter of 30 mm, and then

hot-rolled at 850 °C into sheets with 3 mm in thickness. The hot-rolled plate was cold-rolled into a sheet with 0.3 mm in thickness, and solution-annealed at 800 °C for 30 min followed by rapid water quenching. The sheet samples after quenching were aged at 450 °C for appropriate time. The aged samples were followed by tensile test and hardness measurements. Vickers hardness (at load of 0.5 kg) of these samples aged at 450 °C for different time was measured by a 430SVD Vickers hardness tester. Flat tensile samples with a gauge length of 50 mm, were machined from the solution-treated sheets and those aged for 3, 10, 16, 30 and 40 h at 450 °C and tested for tensile properties according to the GB/T 228.1–2010 standard.

The specimens for X-ray diffraction experiments, with dimensions of 15 mm × 25 mm × 0.3 mm, were ground to 2000 grade waterproof abrasive paper. The experiments were carried out using a D8 Advance X-ray diffractometer of Bruker with  $K_{\alpha}$  diffraction rays of Cu target at an accelerating voltage of 40 kV, current of 40 mA and step-scanning rate of 40 min<sup>-1</sup>. The direction of X-ray was perpendicular to the rolling plane.

Thin foil samples for TEM observation were prepared from sheet materials. Sheet samples were mechanically polished to 50–60 μm. Discs of 3 mm in diameter punched out from the samples were electropolished using a twin-jet electropolisher, using a solution of 8% perchloric acid and 92% ethanol (volume fraction) at –30 °C and 50 V. The microstructures of the foil samples were observed using a JEM 2100F TEM with an operation voltage of 200 kV.

### 3 Results and discussion

#### 3.1 Material properties

The hardness of the solution-treated Cu–20Ni–20Mn alloy aged at 450 °C is shown in Fig. 1. There is a long incubation period at 450 °C, during which no appreciable change in hardness is observed. Once age

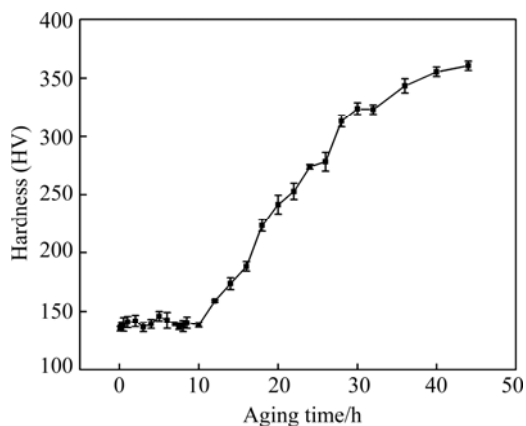


Fig. 1 Hardness of Cu–20Ni–20Mn alloys at aging temperature of 450 °C

hardening is initiated, the increase of hardness is quite rapid when the aging time exceeds more than 10 h. The amplification of the hardness decreases gradually with increasing time, whereas the hardness does not attain the peak value at 450 °C even after aging for 44 h.

The effect of aging time on yield strength, ultimate tensile strength and elongation of Cu–20Ni–20Mn alloy aged at 450 °C is shown in Fig. 2. As can be seen from the curves, there are no appreciable changes in yield strength and ultimate tensile strength in the initial period of aging. However, the yield strength and ultimate tensile strength increase gradually with prolonging the aging time. The yield strength is raised from 177 to 856 MPa and tensile strength from 409 to 942 MPa with increasing aging time from 0 to 40 h. The elongation, however, decreases from 35% in solution-treated condition, to 1.4% when aging at 450 °C for 40 h. The variation in strength and elongation of the alloy is due to the microstructure evolution or precipitation during the aging process of the alloy, which will be discussed in the following section.

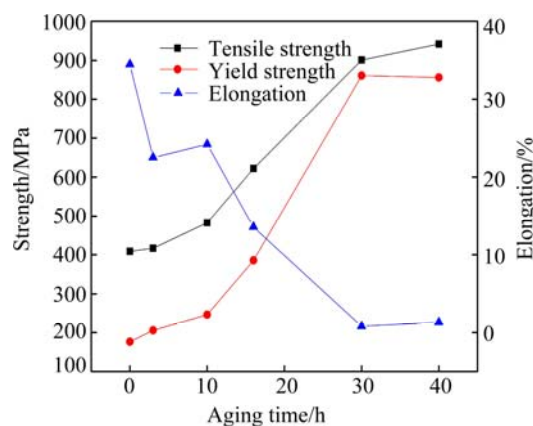
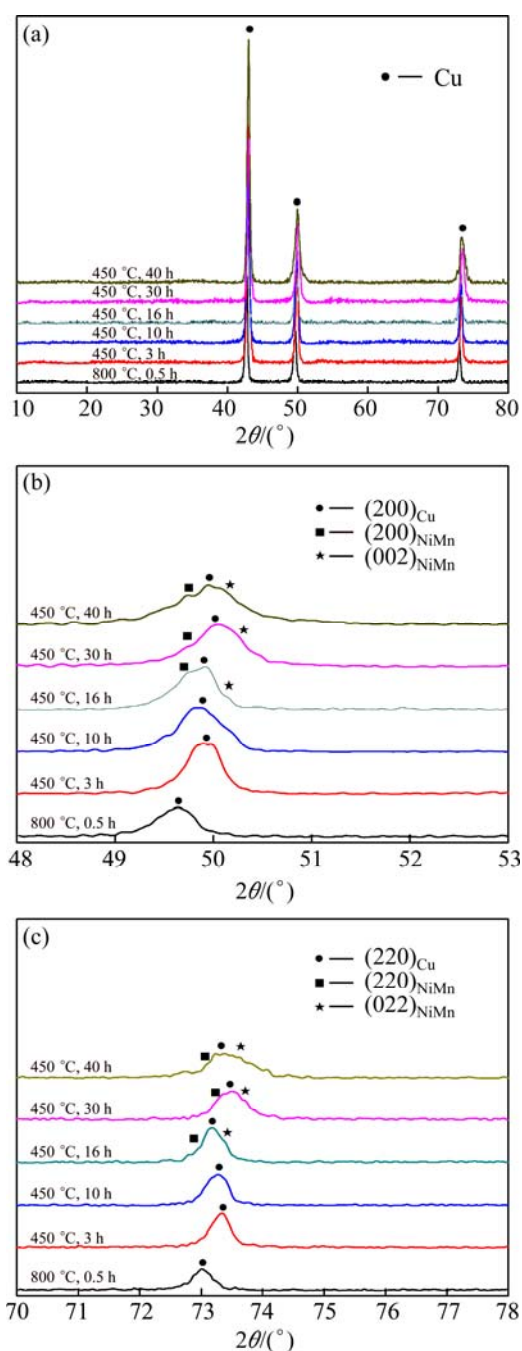


Fig. 2 Strength and elongation of Cu–20Ni–20Mn alloys at aging temperature of 450 °C

#### 3.2 XRD analysis

The XRD patterns of Cu–20Ni–20Mn alloy aged at 450 °C for different time and solution-treated at 800 °C for 0.5 h are shown in Fig. 3. The diffraction patterns in  $2\theta$  ranges of 48°–53° and 70°–78° are respectively magnified in Figs. 3(b) and (c) to reveal the phase transformation during the aging process. It is found that the (200) and (220) peaks of solid solution are gradually widened with prolonging the aging time, and the peaks of ordered FCT phase appear in the vicinity of matrix peak after a long incubation period. The (200)<sub>NiMn</sub> and (002)<sub>NiMn</sub> peaks can be obtained because the appearance of the ordered NiMn phase with FCT symmetry, and the two peaks on both sides of the (200)<sub>Cu</sub> indicate that the lattice parameters of the copper matrix and ordered phase by Bragg equation are very close, which is in good agreement with the analysis of TEM.



**Fig. 3** XRD patterns of Cu–20Ni–20Mn alloy aged at 450 °C for different time and solution-treated at 800 °C for 0.5 h in different  $2\theta$  ranges: (a)  $10^\circ$ – $80^\circ$ ; (b)  $48^\circ$ – $53^\circ$ ; (c)  $70^\circ$ – $78^\circ$

### 3.3 Microstructure

The TEM image and the corresponding selected area electron diffraction (SAED) patterns of specimen aged at 450 °C for 3 h are shown in Fig. 4. A few dislocations without spinodal structures are observed in the matrix, as shown in Fig. 4(a), which is supported by the diffraction pattern in Fig. 4(b). The pattern is a typical face-centered cubic (FCC) pattern for a foil normal of  $[011]_{\text{FCC}}$ .

Figure 5 shows the TEM and the corresponding selected area electron diffraction patterns of specimen aged at 450 °C for 16 h. The intragranular structure is significantly different from that in Fig. 4(a). A large number of finely dispersive distributed particles are shown in Fig. 5(a), and the images of the particles resemble butterflies or coffee beans with a line in the center of no contrast. The micrograph indicates that particle geometry is approximately spherical, which is coherent with the matrix [12]. Furthermore, lattice-strain effects around larger precipitates appearing as rings without a line of no contrast can be observed in Fig. 5(a). Besides the matrix spots, there are some weak spots appearing in the SAED pattern from Fig. 5(b). It should be noted that this intensity is hardly visible in the electron microscope and that it can only be recorded by overexposing the SAED pattern, as seen from the size of the basic reflections. The new weak spots reveal that the ordered phase is present, and the precipitate particles may belong to  $L1_0$  structure. Compared with the specimens aged at 450 °C for 3 h, the hardness and strength of the alloy aged for 16 h increase significantly due to the appearance of the precipitate particles.

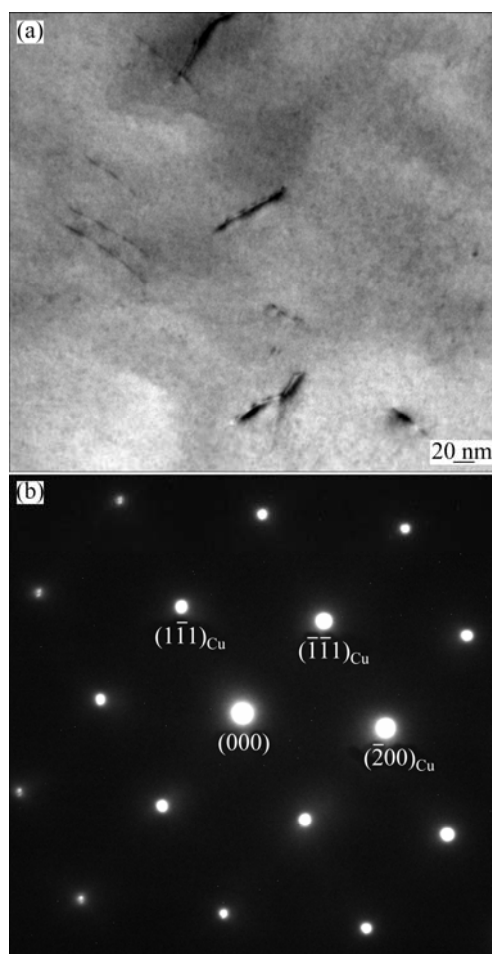


**Fig. 4** TEM image (a) and  $[011]_{\text{FCC}}$  SAED pattern (b) of Cu–20Ni–20Mn alloy aged at 450 °C for 3 h

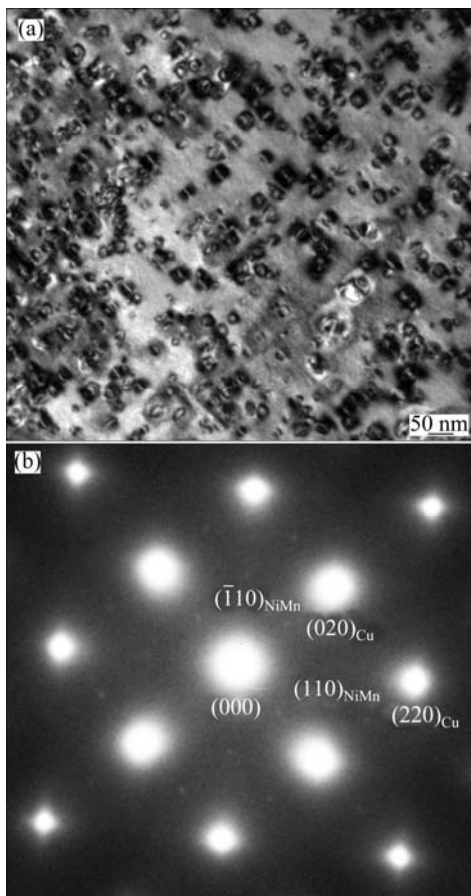


**Fig. 5** TEM image (a) and  $[001]_{\text{FCC}}$  SAED pattern (b) of Cu-20Ni-20Mn alloy aged at 450 °C for 16 h

The bright filed TEM image and the corresponding SAED pattern of specimen aged for 30 h are shown in Fig. 6. With further aging to 30 h, the line of no contrast does not appear in the micrograph (Fig. 6(a)), and discrete precipitate particles have grown to a sufficient size such that coherency strains are evident, as shown in Fig. 6(b). A typical face-centered cubic pattern for a foil normal of  $[001]_{\text{FCC}}$ , with the diffuse spots, is sharpened and extra intensities become visible. Again, the presence of the ordered phase is indicated by the  $(001)_{\text{NiMn}}$  reflection. Contrast to the SAED pattern after being aged for 16 h, the spots at intermediate position such as  $(110)$  spot are extinct. It is further confirmed that the ordered phase is  $L1_0$  structure with FCT symmetry. Different zone axes correspond different SAED patterns for ordered  $L1_0$  single crystals, For example, the  $(110)$  spot appears and  $(100)$  spot vanishes in the  $[001]_{L1_0}$  pattern. Therefore, the SAED pattern mainly consists of  $[001]_{\text{FCC}}$  pattern,  $[100]_{L1_0}$  pattern and  $[010]_{L1_0}$  pattern. The intensity of the spots at  $L1_0$   $(110)$  position is too weak to be observed since the quantity of ordered phase  $[001]_{L1_0}$  pattern on the specific orientation is too small. The orientation relationship between the copper matrix and the ordered  $\text{NiMn}$  phase ( $L1_0$  phase) is:  $(020)_{\text{Cu}}//$

$(001)_{\text{NiMn}}$  and  $[001]_{\text{Cu}}//[010]_{\text{NiMn}}$ . Combined with the thermodynamic model in Cu-Ni-Mn alloy [5], the precipitation is the ordered NiMn phase with FCT structure.

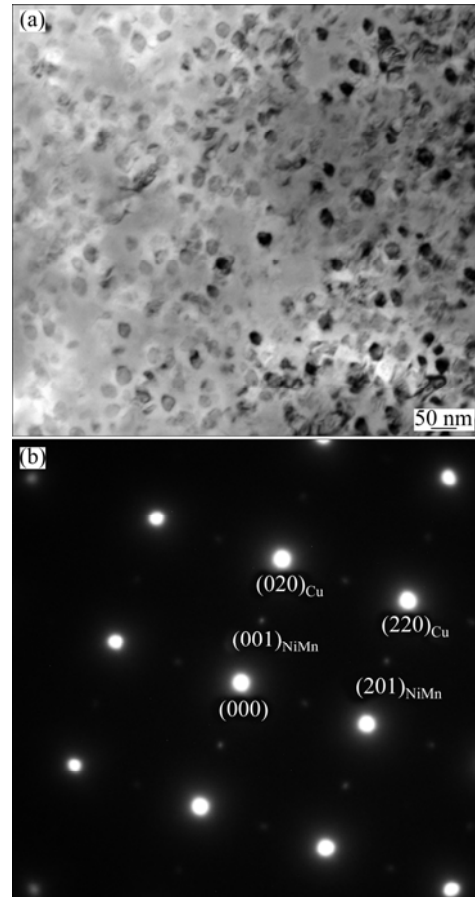


**Fig. 6** TEM image (a) and  $[001]_{\text{FCC}}$  SAED pattern (b) of Cu-20Ni-20Mn alloy aged at 450 °C for 30 h

The hardness and strength properties of the alloys are greatly influenced by the microstructural changes that take place during the aging treatments [13–16]. A long incubation time prior to general precipitation is observed in aged samples. The microstructure of Cu-Ni-Mn alloy aged at 450 °C for 3 h has no significant change, corresponding to the hardness and strength, of which spinodal decomposition structure cannot be observed. The spinodal decomposition can take place by uphill diffusion instead of nucleation and growth, and the transformation rate of spinodal decomposition is very high [17]. Therefore, the spinodal decomposition may not occur during aging process at 450 °C. The main precipitation mechanism of the alloy aged at 450 °C could be nucleation and growth, indicated by the discrete nucleation sites and ordered NiMn phases observed by TEM in Cu-Ni-Mn alloy aged for 16 h. The average size of particles without a line of no contrast aged at 450 °C for 16 h is about 19 nm, which is larger than the real average size of precipitate because the sizes of

particles with a line of no contrast cannot be measured. The average size of particles aged for 30 h statistically measured by TEM is about 25 nm, indicating that the precipitates are coarsened with prolonging aging time. And the tensile strength and hardness are evidently improved because the sizes of the coherent FCT-NiMn phases are large. This indicates that the strength is mainly affected by the precipitation of the ordered coherent NiMn phase.

## 4 Conclusions

1) The Cu-20Ni-20Mn alloy is a precipitation hardening alloy. The dominating precipitation process of the alloy aged at 450 °C can nucleate and grow, and no spinodal decomposition structure is observed in the initial stage of aging.

2) There is a long incubation period of nucleation, growth and coarsening for Cu-20Ni-20Mn alloy at the initial 10 h and its mechanical properties do not change obviously. Subsequently, the tensile strength, yield strength and hardness rapidly increase, the maximum yield strength and tensile strength can reach 856 MPa and 942 MPa for the alloy aged at 450 °C for 40 h, respectively.

3) Precipitate phase is the ordered NiMn phase with  $L1_0$  type FCT structure maintaining coherent with the matrix. And the ordered phase has an orientation relationship with the matrix:  $(020)_{Cu} // (001)_{NiMn}$  and  $[001]_{Cu} // [010]_{NiMn}$ .

## References

- [1] BOEGEL A, OHLA K, MUELLER H R. Copper-nickel-manganese alloy, products made therefrom and method of manufacture of products therefrom: United States, US 6811623B2 [P]. 2004-11-02.
- [2] BOBYLEV A V. Microhardness of Cu-Ni-Mn alloy reduced by etching reagents [J]. Metal Science and Heat Treatment, 1962, 2(1): 49-50.
- [3] RONDOT D, MIGNOT J. The study of the initial stages of structural transformation in a Cu-20Ni-20Mn alloy [J]. Acta Metallurgica, 1978, 26(2): 217-222. (in French)
- [4] BAZHENOV V E. Phase diagram of the Cu-Ni-Mn system [J]. Russian Journal of Nonferrous Metals, 2013, 54(2): 171-177.
- [5] SUN Wei-hua, XU Hong-hui, LIU Shu-hong, CHEN Hai-lin, ZHANG Li-jun, HUANG Bai-yun. Experimental investigation and thermodynamic modeling of the Cu-Mn-Ni system [J]. Calphad, 2009, 33(4): 642-649.
- [6] MIETTINEN J. Thermodynamic description of the Cu-Mn-Ni system at the Cu-Ni side [J]. Calphad, 2003, 27(2): 147-152.
- [7] PIKUNOV M V, SIDOROV E V. Structure of the phase diagram of the Cu-Ni-Mn system [J]. Steel in Translation, 2008, 38(5): 351-354.
- [8] BAZHENOV V E, PIKUNOV M V. Temperature minimum line in the Cu-Ni-Mn phase diagram [J]. Steel in Translation, 2010, 40(3): 225-228.
- [9] ZHANG Wei-bin, DU Yong, ZHANG Li-jun, XU Hong-hui, LIU Shu-hong, CHEN Li. Atomic mobility, diffusivity and diffusion growth simulation for FCC Cu-Mn-Ni alloys [J]. Calphad, 2011, 35(4): 367-375.
- [10] PAN Qi-han. A highly elastic Cu-20Ni-20Mn alloy [J]. The Chinese Journal of Nonferrous Metals, 1996, 6(4): 91-95. (in Chinese)
- [11] SHAPIRO S, TYLER D E, LANAM R. Phenomenology of precipitation in copper-20 Pct nickel-20 Pct manganese [J]. Metallurgical Transactions, 1974, 11(5): 2457-2469.
- [12] JANSSENS K J F, BIEST O V, VANHELLEMONT J, MAES H E. Assessment of the quantitative characterization of localized strain using electron diffraction contrast imaging [J]. Ultramicroscopy, 1997, 69(3): 151-167.
- [13] WANG Kun, LIU Ke-fu, ZHANG Jing-bo. Microstructure and properties of aging Cu-Cr-Zr alloy [J]. Rare Metals, 2014, 33(2): 134-138.
- [14] XIAO Xiang-peng, XIONG Bai-qing, WANG Qiang-song, XIE Guo-liang, PENG Li-jin, HUANG Guo-xing. Microstructure and properties of Cu-Ni-Si-Zr alloy after thermomechanical treatments [J]. Rare Metals, 2013, 32(2): 144-149.
- [15] ZHRABYAN D, MILKEREIT B, SCHICK C, KESSLER O. Continuous cooling precipitation diagram of high alloyed Al-Zn-Mg-Cu 7049A alloy [J]. Transactions of Nonferrous Metals Society of China, 2014, 24(7): 2018-2024.
- [16] PENG Li-jun, XIONG Bai-qing, XIE Guo-liang, WANG Qiang-song, HONG Song-bai. Precipitation process and its effects on properties of aging Cu-Ni-Be alloy [J]. Rare Metals, 2013, 32(4): 332-337.
- [17] HAO Xin-jiang, LI Hong-xiao, ZHAO Gang, HAO Shi-ming. Effect of prior deformation on aging process in a Cu-30Ni-25Fe spinodal alloy [J]. Journal of Materials Science and Technology, 1999, 15(6): 519-522.

# 时效过程中 Cu-20Ni-20Mn 合金的显微组织演变及性能

谢伟滨, 王强松, 米绪军, 解国良, 刘冬梅, 高学成, 李洋

北京有色金属研究总院 有色金属材料制备加工国家重点实验室, 北京 100088

**摘要:** 通过 X 射线衍射(XRD)和透射电镜(TEM)研究 Cu-20Ni-20Mn 合金在 450 °C 时效过程中的显微组织及相转变, 并对时效后合金的抗拉强度、屈服强度和硬度进行分析。结果表明, 时效开始阶段存在一个很长的孕育期, 此时合金的强度和硬度没有明显变化。随着时效时间的延长, 有序的面心四方结构 (FCT) NiMn 相在晶粒中形核并长大。随着有序 FCT 结构相尺寸的增加, 合金硬度和强度提高并达到极大值。在 450 °C 时效 40 h 后合金强度达到 942 MPa。由有序 FCT 结构 NiMn 相所产生的沉淀强化是合金主要的时效强化因素。

**关键词:** Cu-Ni-Mn 合金; 显微组织; 力学性能; 有序相

(Edited by Wei-ping CHEN)